Available online at www.sciencedirect.com
ScienceDirect
Journal of the European Ceramic Society 30 (2010) 221–225
www.elsevier.com/locate/jeurceramsoc

Correlation between impedance spectra of bulk ceramics and films with in-plane configuration

A.A.L. Ferreira [a], J.C.C. Abrantes [a,b,*], J.R. Frade [b]

[a] *UIDM, ESTG, Polytechnic Institute of Viana do Castelo, Portugal*
[b] *CICECO, Ceramic and Glass Engineering Department, University of Aveiro, Portugal*

Available online 29 July 2009

Abstract

Strontium titanate is an interesting model electroceramics with grain boundary controlled properties. However, the relative role of grain boundaries may be significantly different in bulk ceramics and in films. Under oxidising conditions, impedance response of bulk ceramics can be described by series association of bulk and grain boundary contributions, which are distinguished based on major differences in relaxation frequencies. This allows de-convolution over relatively wide temperature ranges with standard impedance meters. In this case, one finds reasonably good correlations between microstructural effects and grain boundary behaviour. However, one finds major differences between those spectra and corresponding impedance spectra obtained for in-plane measurements of films. This may be partially accounted for by major increase in the equivalent thickness/area ratio as well as microstructural changes. In addition, the substrate may affect the results by significant leakage, and by stray capacitance effects exerted by a combination of substrate and experimental equipment.

Keywords: Strontium titanate; Films; Impedance spectroscopy; In plane; Stray capacitance

1. Introduction

The applicability of strontium titanate materials as electrical or electrochemical devices has been demonstrated [1–4], based on detailed studies of their transport properties [5–8], including descriptions of microstructural effects based on de-convolution of bulk and grain boundary behaviour [9,10]. Most of these applications are indeed processed as films obtained by physical deposition [11] or more conventional screen printing [12], and are the basis for multilayered devices or systems. Processed films also allow one to study unique features such as two dimensional configurations, texturing, nanostructuring, interface design, etc., which cannot be obtained by bulk ceramic processing. Yet, many experimental studies often rely on the electrical characterization of ceramics pellets. Thus, one should be careful about misinterpretations of differences between the electrical response of films and bulk ceramics.

The most obvious difference between bulk ceramics and films is the geometric factor, i.e., the area:thickness ratio. For ceramic samples with typical thickness in the order of 1–2 mm, and diameter 5–20 mm, one predicts values of geometric factor in the range 10–300 mm. The corresponding geometric factor for films may be orders of magnitude higher for measurements across the film, or orders of magnitude lower for in-plane electrode configurations. For example, on assuming film thickness in the order of 1–10 μm, with in plane 10 mm wide electrodes, and for 5 mm inter-electrode distance, one expects values of geometric factor in the range 5–50 μm, i.e., at least 3 orders of magnitude smaller than for bulk samples. This implies much higher impedance and much lower capacitance values for in-plane measured films. The corresponding geometric factor for relatively thick substrates with in-plane electrode configuration should be intermediate between the geometric factors for pellets with parallel electrodes and films with in-plane configuration. Concerns about in-plane measurements must, indeed, be taken into account. This is important to avoid misinterpretations of the electrical behaviour of titanate films and a variety of electroceramic films deposited on different substrates (e.g. [13]), and to monitor the behaviour of multilayered devices, or electrochemical cells by electrical or electrochemical measurements.

The purpose of this work was to study correlations between the impedance response of bulk ceramics and films, including effects exerted by the substrate, even for cases when the

* Corresponding author at: UIDM, ESTG, Polytechnic Institute of Viana do Castelo, 4900-348 Viana do Castelo, Portugal.
E-mail address: jabrantes@estg.ipvc.pt (J.C.C. Abrantes).

0955-2219/$ – see front matter © 2009 Elsevier Ltd. All rights reserved.
doi:10.1016/j.jeurceramsoc.2009.06.017

resistivity of the substrate is orders of magnitude higher than for the film, and for large differences between the permittivity of the film and substrate materials. Additional limitations might be imposed by the internal characteristics of the impedance meter, including its stray capacitance [14]. $SrTiO_3$ was selected as a model material to correlate electrical measurements for bulk ceramics and films with in-plane configuration.

2. Experimental

Powders of $SrTiO_3$ were prepared by solid state reaction using high purity precursors $SrCO_3$ (BDH-30275) and TiO_2 (Merck-1.00808), after mixing in nylon container with YSZ spheres, for 2 h, calcining at 1100 °C for 15 h, and then milling again to destroy agglomerates and to minimize heterogeneities. These powders were used to prepare ceramic samples, to deposit thin layers on dense alumina substrates, by screen printing, and to prepare $SrTiO_3$ ceramic samples. Ceramic samples were obtained by uniaxially pressing at about 10^8 Pa, and sintering at 1200–1400 °C to obtain porous samples, or higher temperatures to obtain nearly fully dense samples. Films were deposited on alumina disks, by screen printing. The serigraphic screen has cord diameter of 123 μm, mesh aperture of 290 μm, depth of 220 μm and open surface of about 49%. The solid to liquid ratio in the suspension was 1.5 g/cm^3, and commercial serigraphic oil was used as suspension agent. The screen printed films were fired at temperatures in the range 1300–1500 °C, and for times ranging from 10 min to 10 h. Scanning electron microscopy and microprobe analysis were used for microstructural characterization of bulk ceramics and films, including assessment of their thickness (Fig. 1), and to monitor degradation of films by chemical reactions and/or interdiffusion at excessively high firing temperatures. A commercial Pt paste was used to paint electrodes on sintered pellets and on films with in-plane configuration. The electrical characterization was performed with the impedance meter Hewlett-Packard 4824A in the range of 20 to 1 MHz at temperatures 200–1000 °C, in different atmospheres (i.e., air, N_2, and $5\%H_2 + 95\%N_2$). Electrical measurements were also performed as a function of oxygen partial pressure, using a potentiometric YSZ sensor to monitor the oxygen partial pressures.

3. Results and discussion

SEM microstructures (Fig. 1) show that the relative density of screen printed films increases with firing temperature. The most obvious indication of this is the difference between thickness for films deposited from the same suspension and with identical mesh. Indeed, this affects the differences between electrical measurements (Fig. 2). Measurements on films were obtained with in-plane configuration, and their conductivity was estimated as $L/(AR_{ip}) = L/(w\Delta R_{ip})$, where L is the inter-electrode distance, w is electrode width and Δ is the film thickness. The conductivity results for alumina substrates and dense strontium titanate ceramics were obtained with pellets.

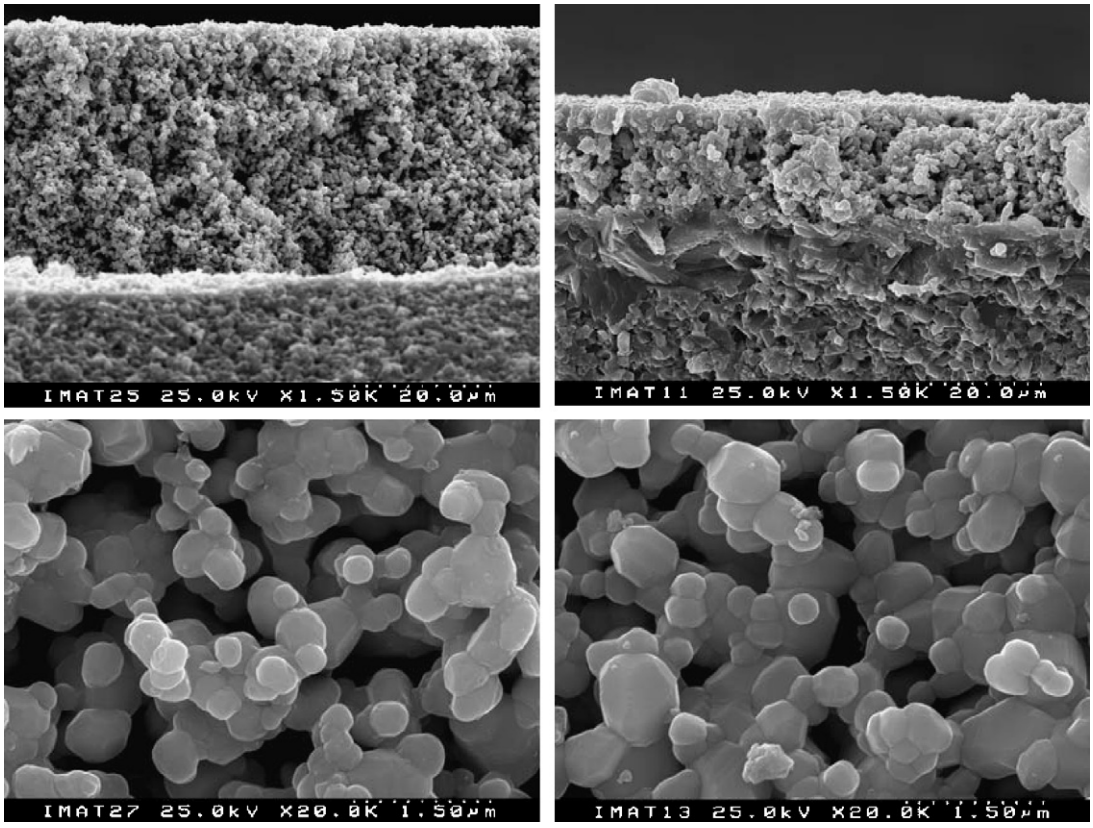

Fig. 1. SEM microstructures of screen printed films fired at 1300 °C (left) and 1400 °C (right).

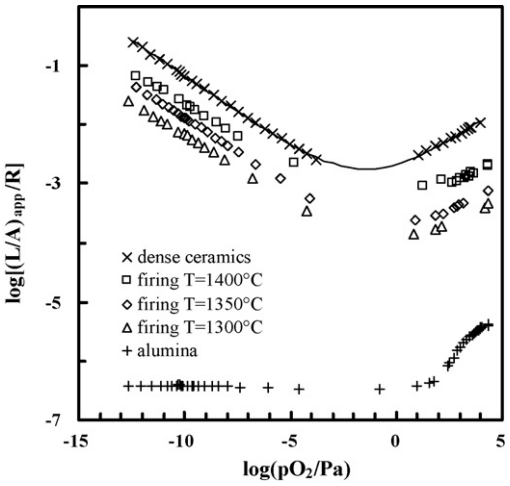

Fig. 2. Electrical characterization performed at 1000 °C for screen printed films fired at 1300 °C (triangles), 1350 °C (diamonds), and 1400 °C (squares). The corresponding conductivity measurements obtained for one dense ceramic strontium titanate sample, and for one alumina pellet are shown as +.

The in-plane measurements of films shown in Fig. 2 suggest the expected transition from n-type to p-type behaviour, as found for the bulk strontium titanate sample. The differences between dense bulk samples and porous films can, indeed, be ascribed to the high porosity of those films. The effects of firing temperature on the densification of films are confirmed by significant differences in resistance, without major changes in n-p transition. Fig. 2 also shows that the conductivity of alumina is orders of magnitude lower than the conductivity of strontium titanate, especially for measurements under reducing conditions, due to the increase in n-type conductivity of strontium titanate. However, the alumina substrate may affect in-plane measurements, as shown in Fig. 3. Note that the differences in resistance obtained for the film and for the substrate are relatively small for measurements in air and in nitrogen. The actual behaviour thus converges to a parallel association of the resistances of film and substrate. The contribution of the alumina substrate increases

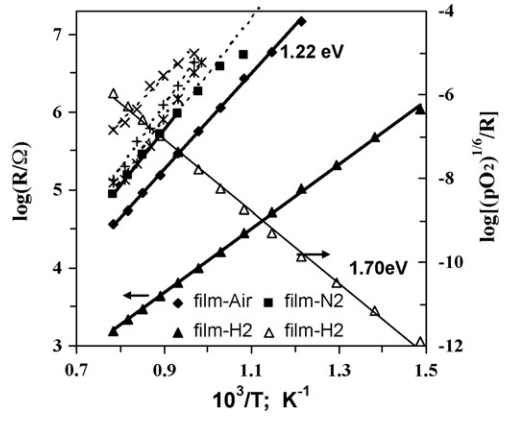

Fig. 3. Temperature dependence of in-plane resistance of screen printed film in air (diamonds), N_2 (squares), and $5\%H_2 + 95\%N_2$ (triangles). The left scale shows the temperature dependence of n-type conductivity after compensating for changes in oxygen partial pressure $\sigma_{n,1} = \sigma_n(pO_2)^{1/6} = (L/A)_{eff}(pO_2)^{1/6}/R$. The corresponding results for alumina substrate are shown as (+), (*) and (x) for measurements in air, N_2, and $5\%H_2 + 95\%N_2$.

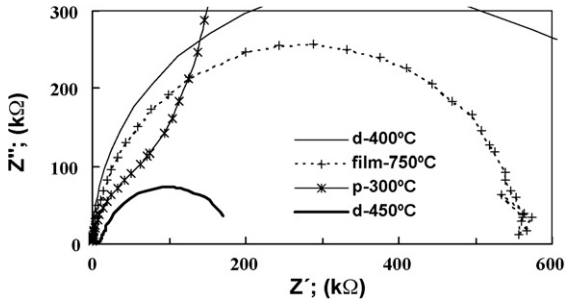

Fig. 4. Impedance spectra of one screen printed film at 750 °C, one dense pellet at 400 and 450 °C, and one porous pellet at 300 °C.

with temperature due to its higher activation energy. Indeed, the interference of the alumina substrate is less critical under reducing conditions due to the increase in n-type conductivity of strontium titanate.

Impedance spectra show further evidence that in-plane measurements of films differ significantly from that of bulk samples (Fig. 4). Though the electrical behaviour of bulk ceramic samples tends to be controlled by resistive grain boundaries, impedance spectra still show clear de-convolution of bulk and grain contributions, mainly for dense samples. On the contrary, the impedance spectra obtained for screen printed films suggest a single microstructural contribution. Though porous ceramic samples still show evidence of the bulk contribution, this reduces to the high frequency shoulder observed in Fig. 4. These effects are consistent with the literature showing that porosity [15] affects the correct de-convolution of impedance contributions of bulk and grain boundaries. The bulk contribution is shown clearer by modulus representations, as demonstrated in Fig. 5. Note that the peak of bulk contributions is displaced to higher frequencies with increasing temperatures and cannot be seen at temperatures above about 450 °C.

Though porosity depresses the bulk peak in modulus representations (Fig. 5), this peak is still obvious for conditions when usual representations of Z″ vs Z′ become unclear. Thus, one attempted to detect the bulk contributions for films by the representations of modulus, as shown in Fig. 6. These results show

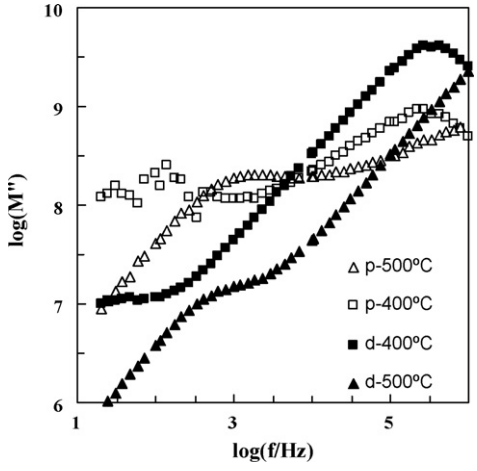

Fig. 5. Modulus vs frequency for porous (open symbols) and dense ceramics (closed symbols) at 400 °C (squares) and 500 °C (triangles).

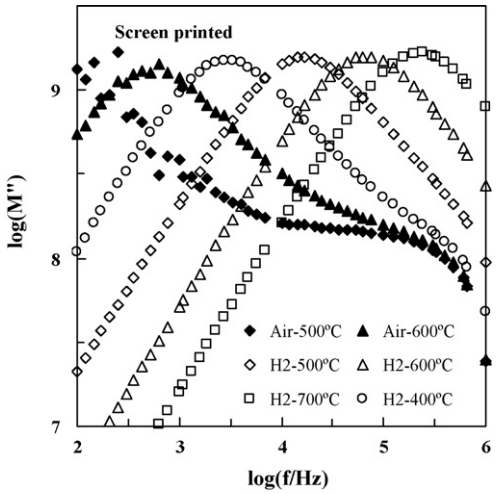

Fig. 6. Modulus vs frequency for screen printed film in air (closed symbols) and under reducing atmosphere 5%H_2–95%N_2.

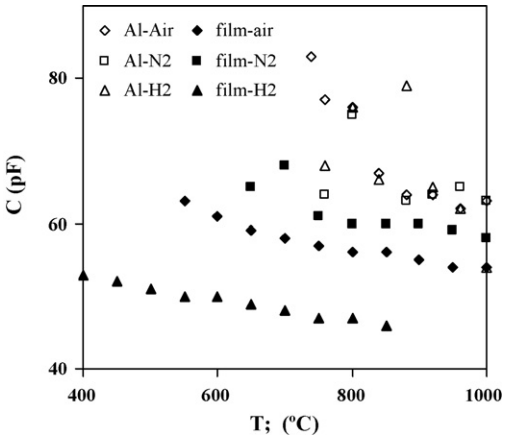

Fig. 7. Capacitance ($C = Q^{1/n}R^{1-n/n}$) values obtained by fitting impedances spectra of screen printed films (closed symbols) in air (diamonds), N_2 (squares) and 5%H_2 + 95%N_2 (triangles). Results for the alumina substrate with in-plane electrodes are also shown (open symbols).

one single main peak, with the additional high frequency shoulder seen at the lowest temperatures, which can still be ascribed to the bulk intragranular behaviour. Indeed, this contribution is very depressed due to the high porosity of the films. The main peak observed by representations of modulus can be ascribed to internal interfaces.

In spite of the differences in amplitude of the main peak of modulus representations in Fig. 5, its location in the frequency range indicates similar temperature dependence for the relaxation frequency. This is consistent with the expected opposite effects of geometric factor $(A{:}L)_{\text{eff}}$ on bulk capacitance $C_B \approx (A/L)_{\text{eff}}\varepsilon_o\varepsilon_r$ and resistance $R_B \approx \rho/(A/L)_{\text{eff}}$, yielding the relaxation frequency $f_B = (2\pi R_B C_B)^{-1} \approx (2\pi\varepsilon_o\varepsilon_r\rho_B)^{-1}$, which should be nearly independent of geometry. Thus, the bulk relaxation frequency at 400 °C is slightly above 10^5 Hz for both dense and porous ceramics, and is displaced to values well above 10^6 Hz at 500 °C. Fig. 6 suggests significantly lower relaxation frequency values for films, indicating that the corresponding capacitance values are higher than expected by consideration of changes in geometric factor $(A/L)_{\text{eff}}$. These somewhat surprising differences can be ascribed to stray capacitances imposed by the alumina substrate and/or by the equipment, as shown below. Note that the equipment may impose stray capacitance values well above 10 pF [14].

Though the grain boundary relaxation frequencies might also be somewhat lower for films than for dense ceramics, as found on comparing Figs. 5 and 6, these differences are much smaller than for the bulk relaxation frequency, probably because the actual grain boundary capacitance values are close to the upper limit imposed by the combined stray capacitances of the alumina substrate and measuring equipment, as shown in Fig. 7.

The combined effects of stray capacitances of alumina substrate and equipment can also explain the differences between impedance spectra obtained for porous samples and films, including the representations of modulus (Figs. 5 and 6). A reasonable demonstration is shown in Fig. 8, which compares the impedance data for the porous ceramic sample at 450 °C, with the behaviour predicted for porous films on assuming parallel stray capacitance values $C_{\text{stray}} = 1$, 10 and 10^2 pF. It is assumed that the microstructural characteristics (average grain size, porosity, etc.) of the film resemble those of the porous sample. One assumed typical ranges for film thickness ($\Delta = 20$ μm), electrode width $w = 10$ mm, and interelectrode distance $L = 5$ mm, yielding a geometric $A{:}L = w\Delta/L$ of about 40 μm for the film, which is much smaller than the corresponding values for a measured porous sample ($A{:}L = 13$ mm). On considering these geometric factors one thus estimated the true impedance response of the film and then simulated the in-plane response for parallel association with the alumina substrate, by taking into account its resistance also measured with in-plane electrodes, $R_{\text{al}} = 0.033\exp(1.89 \times 10^4/T)\,\Omega$. Fig. 8 shows simulations for different values of stray capacitance $C_{\text{stray}} = 1$, 10 and 10^2 pF, to demonstrate that the bulk shoulder is progressively lowered as the stray capacitance is increased; this resembles differences between modulus representations of porous ceramics (Fig. 5) and films (Fig. 6).

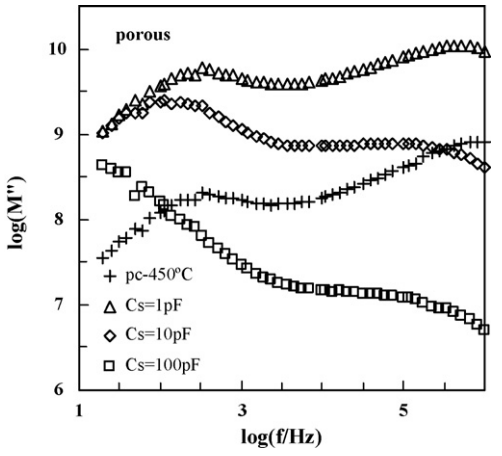

Fig. 8. Modulus representation of porous ceramic sample at 450 °C (+) and the corresponding predictions for a screen printed film 10 mm wide and 20 μm thick film, with 5 mm inter-electrode distance, for identical porosity and grain size, in parallel with one stray parallel capacitance $C_{\text{stray}} = 1$ pF (triangles), 10 pF (circles) and 100 pF (squares).

4. Conclusions

In spite of major differences in resistivity (by orders of magnitude), the in-plane measurements of strontium titanate films are still affected by alumina substrates, even for relatively thick films. In addition, the dielectric response is very different from the corresponding behaviour of strontium titanate ceramics, including porous samples.

Modulus representations obtained for films usually show a single contribution which should be ascribed to internal interfaces. The bulk behaviour is only revealed by a shoulder in the high frequency range, at the lowest measuring temperatures.

Differences between ceramic samples and films are ascribed to the interference of parallel stray capacitances imposed by the alumina substrate and/or measuring equipment, thus distorting the expected behaviour for microstructural contributions with capacitance values in the order of 10 pF or lower.

The actual electrical response obtained for films with in-plane measurements is reasonably similar to simulated predictions for parallel association of films with one additional data stray capacitance.

Acknowledgement

This work was partially supported by FCT, Portugal, under Project REEQ/710/CTM/2005.

References

1. Gerblinger, J. and Meixner, H., *Sens. Actuators B*, 1991, **4**, 99–102.
2. Menesklou, W., Schreiner, H. J., Hardtl, K. H. and Ivers-Tiffée, E., High temperature oxygen sensors based on doped $SrTiO_3$. *Sens. Actuators*, 1999, **B59**, 184–189.
3. Meyer, R. and Waser, R., *Sens. Actuators B*, 2004, **101**, 335–345.
4. Bayraktar, D., Diethelm, S., Holtappels, P., Graule, T. and Van Herle, J., *J. Solid State Electrochem.*, 2006, **10**, 589–596.
5. Chan, N. H., Sharma, R. K. and Smith, D. M., Non-stoichiometry in $SrTiO_3$. *J. Electrochem. Soc.*, 1981, **128**, 1761–1769.
6. Balachandran, U. and Eror, N. G., Electrical conductivity in strontium titanate. *J. Solid State Chem.*, 1981, **39**, 351–359.
7. Denk, I., Munch, W. and Maier, J., Partial conductivities in $SrTiO_3$: bulk polarization experiments, oxygen concentration cell measurements and defect chemical modelling. *J. Am. Ceram. Soc.*, 1995, **78**, 3265–3272.
8. Moos, R. and Härdtl, K. H., Defect chemistry of donor-doped and undoped strontium titanate ceramics between 1000 °C and 1400 °C. *J. Am. Ceram. Soc.*, 1997, **80**(10), 2549–2562.
9. Denk, I., Claus, J. and Maier, J., Electrochemical investigations of $SrTiO_3$ boundaries. *J. Electrochem. Soc.*, 1997, **144**, 3526–3535.
10. Abrantes, J. C. C., Labrincha, J. A. and Frade, J. R., Applicability of the brick layer model to describe the grain boundary properties of strontium titanate ceramics. *J. Eur. Ceram. Soc.*, 2000, **20**, 1603–1609.
11. Gerblinger, J., Hausner, M. and Meixner, H., Electric and kinetic properties of screen printed strontium titanate films at high temperatures. *J. Am. Ceram. Soc.*, 1995, **78**, 1451–1456.
12. Gerblinger, J. and Meixner, H., Electrical conductivity of sputtered films of strontium titanate. *J. Appl. Phys.*, 1990, **67**, 74539.
13. Burriel, M., Santiso, J., Rossell, M. D., van Tendeloo, G., Figueras, A. and Gracia, G., Enhanced total conductivity of $La_2NiO_4 + d$ epitaxial thin films by reducing thickness. *J. Phys. Chem.*, 2008, **112**, 10982–10987.
14. Abrantes, J. C. C., Peres-Coll, D., Núñez, P. and Frade, J. R., On the use of multichannel data acquisition of impedance spectra. *Ionics*, 2003, **9**, 370–374.
15. Steil, M. C., Thevenot, F. and Kleitz, M., Densification of yttria stabilized zirconia: impedance spectroscopy analysis. *J. Electrochem. Soc.*, 1997, **144**, 390–398.